

Probing the Missing Baryons via kSZ Stacking

Han Miao¹, Wei-Peng Lin^{1,2} and Peng-Jie Zhang^{1,3}

¹ Key Laboratory for Research in Galaxies and Cosmology, Shanghai Astronomical Observatory, Shanghai 200030, China; miaohan@shao.ac.cn

² School of Physics and Astronomy, Sun Yat-Sen University, Guangzhou 510275, China

³ Center for Astronomy and Astrophysics, Department of Physics and Astronomy, Shanghai Jiao Tong University, Shanghai 200240, China

Received 2015 October 13; accepted 2015 November 4

Abstract Kinetic Sunyaev-Zel'dovich (kSZ) stacking has great potential to become a powerful probe of missing baryons, due to advances in CMB experiments and galaxy surveys. In this paper, we study kSZ stacking in hydrodynamic simulations with different gas physics. We quantify the kSZ stacking signal as a function of halo mass, redshift and projection depth. We compare between different simulations to estimate the impact of gas physics such as cooling and supernova feedback. Furthermore, we measure the contribution from warm-hot intergalactic medium (WHIM), which is believed to be the reservoir for most, if not all, missing baryons. We find that the WHIM contribution is significant, at the level of $\sim 10\%$ – 70% , depending on the angular separation from the stacked halos and other factors. However, contribution from the intracluster medium along the line of sight is in general non-negligible. This complexity requires more detailed and comprehensive analysis on probing the missing baryons with kSZ stacking.

Key words: cosmology: theory — large scale structure — kinetic Sunyaev-Zel'dovich effect — missing baryons

1 INTRODUCTION

The Sunyaev-Zel'dovich (SZ) effect (Zeldovich & Sunyaev 1969; Sunyaev & Zeldovich 1970, 1972, 1980) has a unique advantage for probing missing baryons (Fukugita et al. 1998; Bregman 2007). All free electrons contribute to the inverse Compton scattering against cosmic microwave background (CMB) photons and therefore contribute to the SZ effect. Since the majority of baryons are ionized and due to their charge neutrality, the SZ effect looks promising as an *unbiased* probe of baryons in the universe after reionization. In particular, since a significant fraction of missing baryons are believed to be in the form of warm-hot intergalactic medium (hereafter WHIM) with intermediate density and temperature (Cen & Ostriker 1999; Davé et al. 2001; Cen & Ostriker 2006), the SZ effect can act as a promising probe of WHIM.

Depending on the source of energy responsible for inverse Compton scattering, the SZ effect can be classified into two major types, the thermal SZ (tSZ) effect and the kinetic SZ (kSZ) effect. The two differ in their sensitivities to the missing baryons. For the tSZ effect, the contribution is proportional to the electron pressure and therefore the contribution is dominated by hot and dense intracluster medium (ICM). The contribution from gas with overdensity less than 100 is only of the order 10% or less, de-

pending on the angular scale (e.g. White et al. 2002). This severely limits its capability of probing WHIM.

On the other hand, the kSZ effect is in principle more promising. This effect is proportional to the product of electron density and velocity. At large scale, velocity and density are only weakly coupled. Therefore we expect the contribution of each gas component is roughly proportional to its mass fraction. For this argument, we expect that WHIM can contribute of the order 50% of the kSZ signal, making the kSZ effect much more sensitive to WHIM than the tSZ effect. The exact value depends on many factors, such as the statistics used for the analysis (e.g. the kSZ power spectrum, the pairwise momentum, the kSZ stacking, higher order statistics, etc.). Quantifying this contribution is the major motivation of this paper.

The kSZ effect is being detected by various existing experiments and significant improvement in kSZ measurement is expected in the future. In 2012, the ACT experiment (Hand et al. 2012) first reported the detection of the kSZ pairwise momentum of luminous red galaxies (LRGs) at about a 4σ confidence level. The detection of the kSZ effect from a single cluster was reported by Sayers et al. (2013). This object is estimated to have an extraordinarily large peculiar velocity of 3000 km s^{-1} , which makes the otherwise impossible detection possible. Various upper limits on the diffused kSZ power spectrum have been reported/updated by ACT, Planck and SPT (e.g. the ACT

upper limit by Sievers et al. 2013 and the Planck 2015 upper limit (Planck Collaboration et al. 2015a)). Recently, the SPT experiment (George et al. 2015) measured the power spectrum of the diffused kSZ effect at 2.2σ . However, due to contaminations from other sources such as the tSZ effect and cosmic infrared background, these power spectrum measurements suffer from various model uncertainties.

Recently, kSZ stacking was carried out by the Planck team in combination of SDSS low- z galaxies to achieve $\sim 3\sigma$ detection of the kSZ effect (Planck Collaboration et al. 2015b). The detected signal of kSZ stacking has been interpreted as baryons outside of halos (Planck Collaboration et al. 2015b; Hernández-Monteagudo et al. 2015), which are estimated to account for 50% of the total baryon budget (Hernández-Monteagudo et al. 2015). However, interpretation of the stacked signal is complicated. For example, both the WHIM around the stacked halos and ICM along the line of sight (LOS) can contribute to kSZ stacking, due to the large correlation length of peculiar velocity. Existing interpretations of the detected signal adopt a number of simplifications/approximations. Therefore the evidence of missing baryons from the kSZ stacking suffers from significant model uncertainty. More comprehensive and thorough analysis of the stacking statistics is required to robustly interpret the stacking signal.

Instead of a thorough analysis of the complicated observational signals, which would include statistical and systematic errors, in this paper, we will address a simpler, and therefore cleaner question. We will quantify the contribution of WHIM to the perfect kSZ stacking in the sense of being free of any observational noises and systematics through a set of hydrodynamic simulations. This essentially evaluates the optimistic application of kSZ stacking to probe missing baryons. The neglected complexities including various CMB noises and errors in the reconstructed peculiar velocity will further complicate the analysis, and should be included in future analysis.

This paper is organized as follows. In Section 2 we briefly describe the kSZ stacking technique. In Section 3 we outline the simulations used for the stacking and present some details of the analysis. In Section 4 we present the results of stacking from all ionized gas, as a function of halo mass, redshift, angular separation and projection length. Section 5 shows the WHIM contribution to the stacking signal. The discussions and conclusions are presented in Section 6.

2 THE KSZ STACKING TECHNIQUE

The temperature anisotropy of CMB induced by the kSZ effect along the direction \hat{n} is (Sunyaev & Zeldovich 1980)

$$\Theta(\hat{n}) \equiv \frac{\Delta T}{T_{\text{CMB}}} = \int \sigma_T n_e(z, \hat{n}) \left(\frac{\mathbf{v}_e}{c} \cdot \hat{n} \right) a d\chi. \quad (1)$$

Here, n_e is the electron number density, σ_T is the Thomson cross section, and $v_r \equiv \mathbf{v}_e \cdot \hat{n}$ stands for the LOS peculiar velocity of the free electrons. To avoid the minus

sign in the above equation, we have chosen the velocity away from us as negative. $d\chi$ is the radial coordinate interval. For the flat cosmology we adopt, $d\chi = cdz/H(z)$ and $H(z)$ is the Hubble parameter at redshift z . $a = 1/(1+z)$ is the scale factor.

The kSZ effect of a source with optical depth τ is $\Theta \sim 10^{-6}(\tau/10^{-3})$, for a typical radial velocity 300 km s^{-1} . This effect is overwhelmed by the primary CMB. Furthermore, it is often smaller than the tSZ effect or the cosmic infrared background (CIB). Therefore usually we can only detect the kSZ effect statistically. By adding up the kSZ effect associated with many galaxies/clusters/halos, one can boost the kSZ signal. However, since the LOS electron velocity v_r can be either positive or negative and the ensemble average is zero ($\langle v_r \rangle = 0$), a weighting $\propto \hat{v}_r$ has to be included in stacking. Here \hat{v}_r is the estimated v_r . $\langle \hat{v}_r \rangle = 0$ and $\langle \hat{v}_r v_r \rangle > 0$ if the estimation of v_r works. The first property guarantees a clean removal of all scalar contaminations such as primary CMB, tSZ and CIB. The second property guarantees that the kSZ signal stands up after stacking. Usually \hat{v}_r contains significant reconstruction error (e.g. Shao et al. (2011)). However for simulations that we analyze in this paper, we will adopt \hat{v}_r as the averaged electron velocity within the radius of the i -th halo, denoted as v_{halo} . The stacking signal is then

$$w(\theta) \equiv \frac{\sum_i \Theta_i(\theta) \hat{v}_{r,i}}{\sum_i}. \quad (2)$$

Here $\Theta_i(\theta)$ is the kSZ temperature fluctuation associated with the i -th galaxy/cluster/halo and θ is the angular separation from the LOS to the center of stacked halos. We set $\hat{v}_{r,i} = v_{\text{halo}}$ as the LOS velocity estimator from the electrons within the virial radius of i -th galaxy/cluster/halo.

The stacking boosts the kSZ signal against all other sources such as the primary CMB, the tSZ effect and CIB, due to the velocity weighting. However, the stacking signal will still be overwhelmed by fluctuations in the primary CMB. The primary CMB lacks small scale power, so it can be approximated as spatially constant over arcminute scales. Therefore its contamination can be significantly reduced by a compensating filter, namely a window function whose effective area is zero. It will also reduce other contaminations which lack small scale power. The optimal compensating filter was first derived by Haehnelt & Tegmark (1996). After these two steps the Planck team managed to measure the kSZ effect through stacking (Planck Collaboration et al. 2015b). Given the relatively poor angular resolution of Planck, a simplified (and less optimal) filter was adopted.

3 SIMULATION AND ANALYSIS

We perform the kSZ stacking for halos in a controlled set of hydrodynamic simulations with identical cosmology and initial conditions, but different gas physics (adiabatic and radiative runs with/without supernova (SN) wind). These simulations were carried out using the

Table 1 The averaged values of θ_{vir} in arcmin of each of the mass bins at four redshifts are listed. 1' corresponds to the co-moving angular diameter distance of 0.17, 0.41, 0.69 and 1.10 Mpc h^{-1} at the four redshifts, respectively.

| | mass bin 1 | mass bin 2 | mass bin 3 | mass bin 4 |
|------------|------------|------------|------------|------------|
| $z = 0.21$ | 1.35 | 1.98 | 2.90 | 4.21 |
| $z = 0.52$ | 0.54 | 0.79 | 1.16 | 1.68 |
| $z = 1.02$ | 0.30 | 0.44 | 0.64 | 0.92 |
| $z = 2.09$ | 0.18 | 0.26 | 0.38 | 0.51 |

Notes: Here mass bins 1 to 4 stand for the mass range of $[10^{12} M_{\odot} h^{-1}, 10^{12.5} M_{\odot} h^{-1})$, $[10^{12.5} M_{\odot} h^{-1}, 10^{13} M_{\odot} h^{-1})$, $[10^{13} M_{\odot} h^{-1}, 10^{13.5} M_{\odot} h^{-1})$, and $[10^{13.5} M_{\odot} h^{-1}, 10^{14} M_{\odot} h^{-1})$, respectively.

Table 2 The number of halos in each of the mass bins and each redshift are listed.

| | mass bin 1 | mass bin 2 | mass bin 3 | mass bin 4 |
|------------|------------|------------|------------|------------|
| $z = 0.21$ | 36265 | 12474 | 3885 | 1047 |
| $z = 0.52$ | 30360 | 9610 | 2841 | 581 |
| $z = 1.02$ | 22021 | 6250 | 1348 | 196 |
| $z = 2.09$ | 8693 | 1520 | 171 | 5 |

massive parallel code Gadget-2 (Springel et al. 2001; Springel 2005) which incorporates gas physics by means of smoothed particle hydrodynamics with implementation of energy and entropy conservation. The adopted cosmology is a flat Λ CDM cosmology with $\Omega_{\Lambda} = 0.721$, $\Omega_0 = 0.279$, $\Omega_b = 0.0463$, $h = 0.70$ and $\sigma_8 = 0.821$. The cosmic structures evolved from a redshift of 120 to the present epoch in a cubic box with a side length of $L_{\text{box}} = 300$ Mpc h^{-1} , and there are 768^3 dark matter particles and the same number of gas particles in the initial condition. For the adiabatic simulation (denoted as run NR), gas cooling and star formation were not included. For radiative runs, an effective multiphase model was utilized to include gas cooling, star formation and SN feedback. One of these runs only included thermal feedback, rather than feedback from SN wind (denoted as run SFNW), while the other one incorporated both thermal and kinetic feedback with a wind efficiency of 2 which resulted in a supernova wind speed of about 480 km s^{-1} (denoted as run SFWW).

Halos are selected by the Friends-of-Friends (FOF) halo finder. We split halos within $10^{12} M_{\odot}/h < M_{\text{vir}} < 10^{14} M_{\odot}/h$ into four mass bins logarithmically equally spaced. Namely, mass bin 1 to mass bin 4 have mass in the range $M_{\text{vir}}/(M_{\odot}/h) \in (10^{12}, 10^{12.5})$, $(10^{12.5}, 10^{13})$, $(10^{13}, 10^{13.5})$ and $(10^{13.5}, 10^{14})$, respectively. We investigate four redshifts of 0.2, 0.5, 1.0 and 2.0. The numbers of halos in these mass bins and the average virial radius are shown in Tables 1 and 2.

With these simulation data, we can measure $w(\theta)$ and its dependence on the halo mass, redshift and projection length. Only free electrons contribute to the kSZ effect. Therefore in simulations we only stack gas with temperature $T \geq 10^4$ K. We are also able to measure the relative contribution from various gas components such as WHIM.

4 THE SIMULATED KSZ STACKING

Figure 1 shows the result of stacking projected over the whole simulation boxsize $L_{\text{box}} = 300$ Mpc/h, for the adiabatic run. The error bars are measured from projections along the three Cartesian directions. We also carry out a null test to demonstrate that the measured kSZ stacking is indeed statistically significant. For this test we randomly select an LOS as the center and replace $\Theta_i(\theta)$ in Equation (2) as $\Theta(\theta)$ from this center. We then expect no net stacking signal. This is indeed what we find. Figure 1 plots the root mean square (RMS) of this null test, normalized to $N_{\text{halo}} = 1000$. For other values of halo number, the RMS should be scaled by a factor $\sqrt{1000/N_{\text{halo}}}$. With this amount of halos, the signal of kSZ stacking (with the absence of CMB contaminations) is statistically significant for all mass bins.

The stacking signal w decreases with halo mass, as expected. It extends over a wide range of angular separations θ and is not limited within the angular size of the virial radius $\theta_{\text{vir}} \equiv r_{\text{vir}}/D_A(z)$, where $D_A(z)$ is the co-moving angular diameter distance. Peculiar velocity has a large correlation length of tens of Mpc. Therefore all free electrons within tens of Mpc to the halos contribute to the kSZ stacking. In particular, both WHIM near the stacked halos and ICM in distant halos along the LOS contribute.

For a given angular separation θ , where does the signal come from? Figure 2 shows the result at $z = 0.2$ by varying the projection length L_{prop} . It is defined by stacking the gas within the range $r_i - L_{\text{prop}} < r < r_i + L_{\text{prop}}$ where r is the radial distance to the gas (free electrons) and r_i is the distance to the i -th halo. We have shown four cases of $L_{\text{prop}} = 1, 2, 3 \times r_{\text{vir}}$ and $L_{\text{prop}} = L_{\text{box}}/2$. The relative contribution strongly depends on θ . When $\theta \lesssim \theta_{\text{vir}}$, the dominant contribution comes from the gas within the projection depth r_{vir} . When θ increases, contribution from larger distance increases. For example, for mass bin 2, $\theta_{\text{vir}} = 2'$ (Table 1). At $\theta = 2\theta_{\text{vir}}$, the contribution from within r_{vir} is only $\sim 40\%$. At larger θ , even a projection depth $3r_{\text{vir}}$ only captures $\lesssim 60\%$ of the contribution. The situation for other redshifts is similar. For brevity, we only show the case of $z = 0.5$ for the adiabatic run in Figure 3. In general, contribution from large distance can be significant or even dominant, due to the large correlation length of peculiar velocity. This complicates the inversion from the measured stacking signal to the baryon budget (e.g. Hernández-Monteagudo et al. (2015)).

How does the stacking depend on gas physics? Figure 4 compares the results of non-adiabatic runs (with/without SN winds) against the adiabatic run for the lowest mass bin 1, and Figure 5 for mass bin 4. The included gas physics can indeed significantly change the stacking result in complicated ways. First we check the non-adiabatic run with star formation, cooling and SN thermal feedback but no SN winds. Compared with the adiabatic run, the stacking signal is weakened in most regions and $z = 0.2, 0.5$ and 1.0. But towards the halo center, the stacking signal is boosted. In the center, cool-

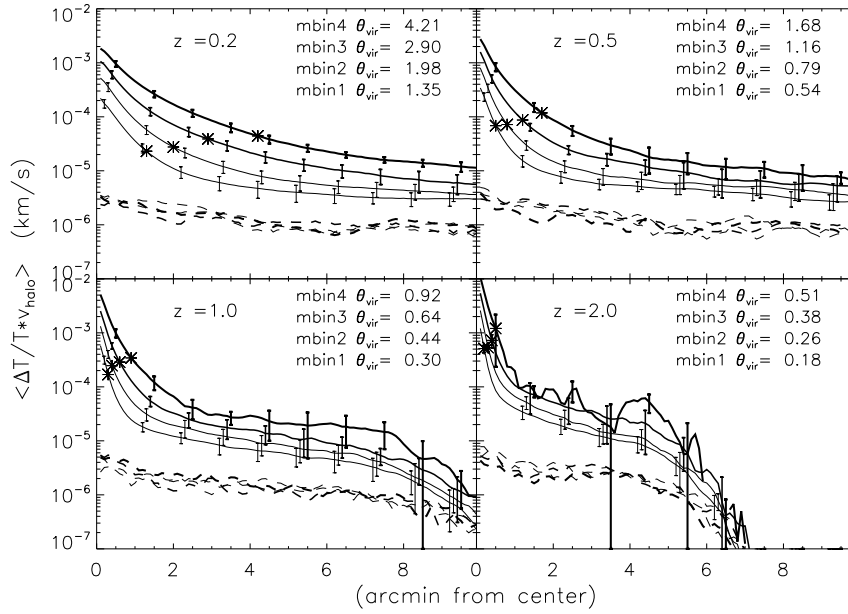


Fig. 1 The weighted kSZ stacking signals in the adiabatic simulation. From top to bottom, the solid lines correspond to the weighted kSZ-stacking signals with decreasing mass. The mass ranges for mass bins 1 to 4 are given in the caption of Table 1, and the stars in the plots are marked as the signal at θ_{vir} . The error bars on top of these solid lines are obtained via projection along the three Cartesian directions. The dashed lines are the RMS of a null test described in the main text, normalized to $N_{\text{halo}}=1000$. These results show that the stacking signal is statistically significant.

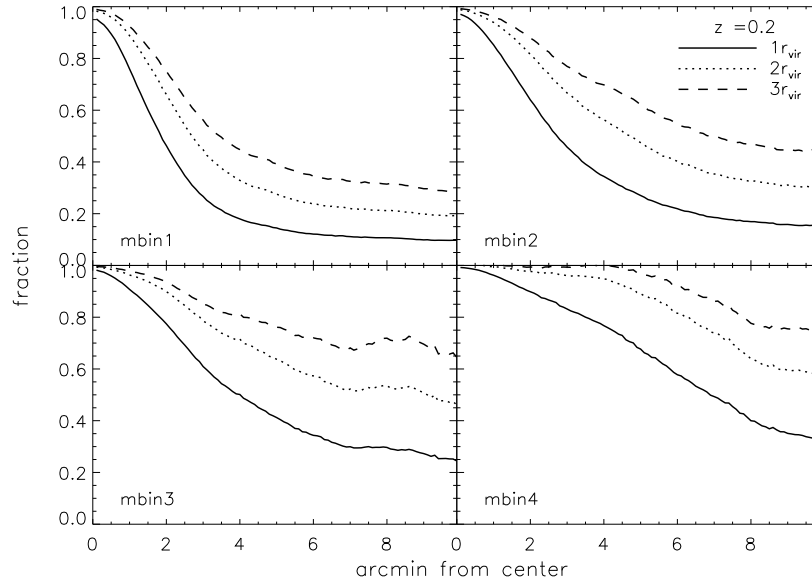


Fig. 2 Contribution of the stacking signal as a function of projection depth ($1r_{\text{vir}}$, solid lines; $2r_{\text{vir}}$, dotted lines and $3r_{\text{vir}}$, dashed lines), at $z = 0.2$ for the adiabatic run. It also serves as the convergence test of the stacking. Along the halo center, most contribution comes from gas within the virial radius. However, a few arcminutes away from the center, the contribution from gas to the distance becomes larger and eventually becomes dominant.

ing dominates (in particular for low mass bins). This not only increases the amount of cool gas, but also increases the amount of ionized gas. We have confirmed these effects by directly checking the halos in these simulations. This later effect boosts the stacking signal around the cen-

ter. But since overall the amount of ionized gas decreases due to cooling, the stacking signal has to be reduced with respect to the non-adiabatic run elsewhere. This explains what we observe at $z = 0.2, 0.5$ and 1.0 in Figures 4 and 5. But at $z = 2$, the stacking signal is boosted at $\theta \gtrsim 2'$.

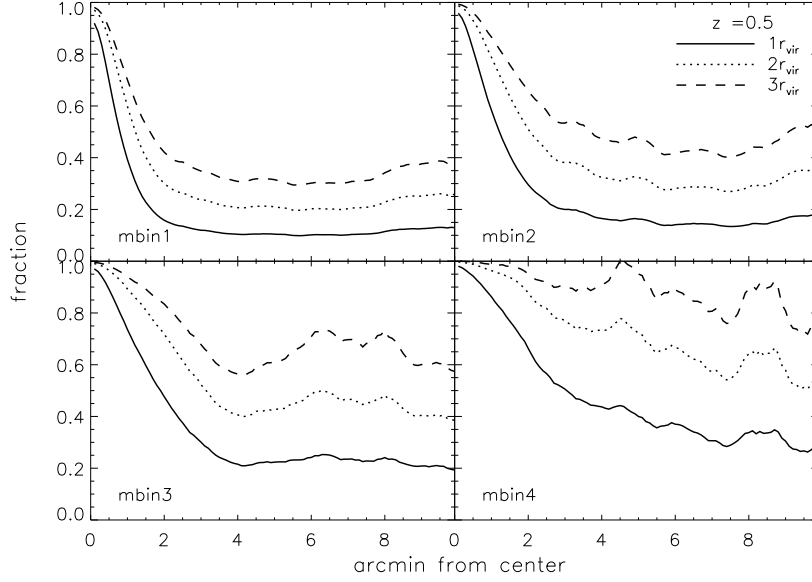


Fig. 3 Same as Fig. 2, but for $z = 0.5$.

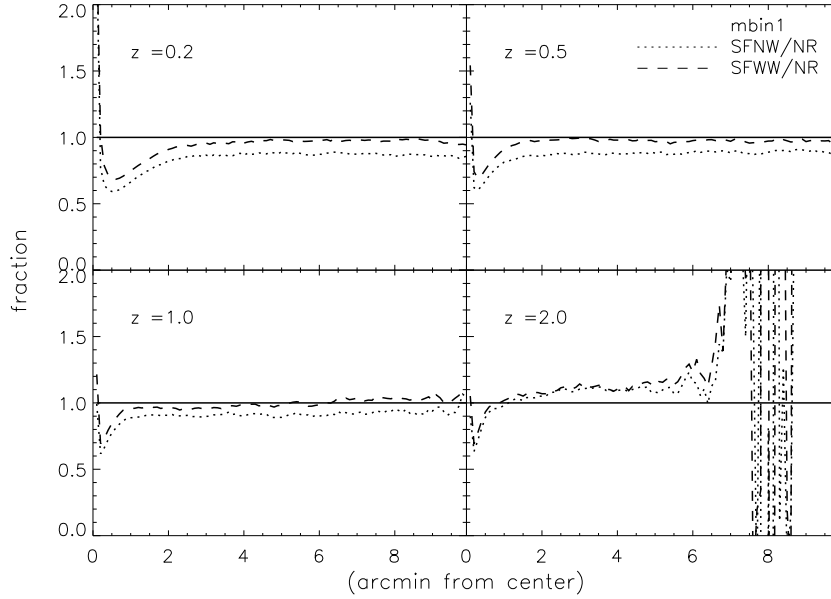


Fig. 4 The ratio of the stacking signal between the non-adiabatic run with/without SN wind and the adiabatic run, for the lowest mass bin 1.

This implies that (thermal) feedback dominates over cooling and therefore there is more ionized gas around small halos compared with the adiabatic run.

With the inclusion of winds, some fraction of gas inside the halos will be displaced outside the halos. This increases the stacking signal at $\theta \gtrsim \theta_{\text{vir}}$ compared to the case with no winds (Figs. 4 and 5). It is due to these competing processes between cooling and dynamical feedback (and perhaps thermal feedback) that the kSZ signal in the non-adiabatic run with winds is almost identical to that of the adiabatic run, for mass bin 1 at $z < 1$ and most of the range

of θ shown in Figure 4. However, this is a coincidence, as can be seen from the case of mass bin 4 (Fig. 5). Halos in this bin are a factor of ~ 30 more massive and therefore have deeper potential wells. The impact of dynamical feedback is limited and hence cannot completely compensate the deficit in gas by cooling. Therefore for mass bin 4, the kSZ signal is weaker in two non-adiabatic runs for most of the range of θ .

Our simulations do not have active galactic nucleus (AGN) feedback, which is known to be important. When including AGN feedback, we expect a further decrease in

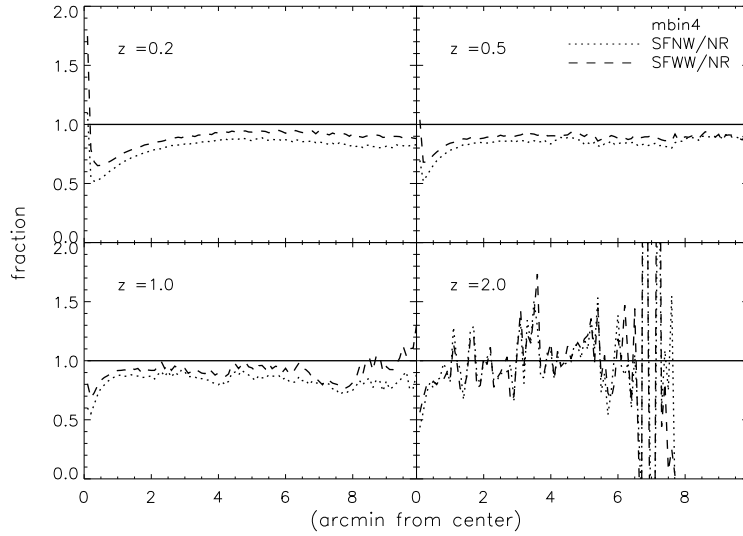


Fig. 5 The ratio of the stacking signal between the non-adiabatic run with/without SN wind and the adiabatic run, for the highest mass bin 4.

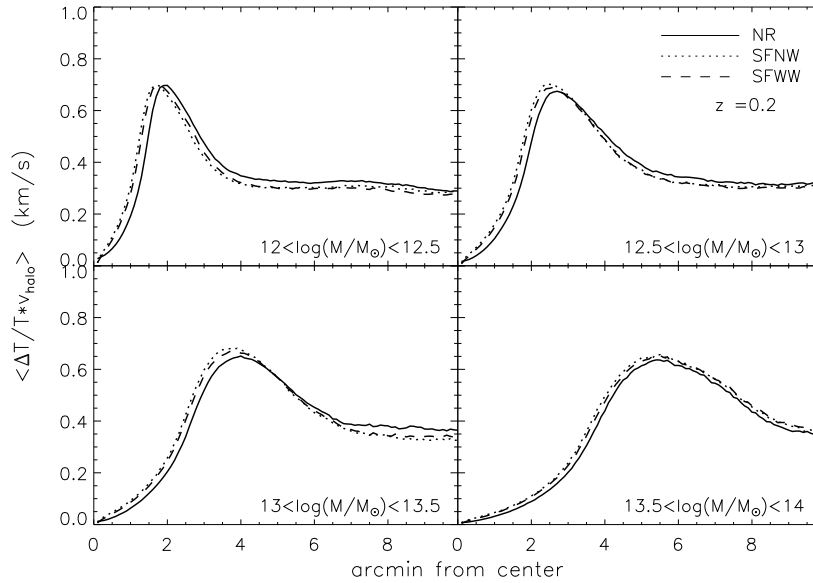


Fig. 6 The fraction of WHIM contribution to the stacking signal at $z = 0.2$. We show the results of all three simulations. Gasphysics has a visible but insignificant impact on the WHIM contribution.

the kSZ stacking signal for halos of all masses and therefore a large impact on gasphysics (e.g. in Figs. 4 and 5). Our overall conclusion is that gasphysics has a non-negligible impact on the kSZ stacking signal.

5 THE WHIM CONTRIBUTION

An important issue to further address is the contribution of WHIM to the stacking signal. This measures the potential of detecting missing baryons with the stacking technique, since WHIM is expected to be the reservoir of at least the majority of missing baryons. WHIM is defined according

to the gas overdensity and temperature, which we have in our simulations. However, the definition varies from literature to literature (e.g. Cen & Ostriker (1999); Davé et al. (2001); Cen & Ostriker (2006)). We treat gas with overdensity in the range $10 < \delta < 100$ and temperature in the range $10^5 \leq T \leq 10^7 \text{K}$ as WHIM. With the overdensity criteria, most of the WHIM is not virialized. It is located beyond the halo virial radius.

Figures 6, 7 and 8 show the fraction of WHIM contribution to the stacking signal at $z = 0.2, 0.5$ and 1.0 for all four mass bins and three simulation runs. The general behavior is that the WHIM contribution first increases with

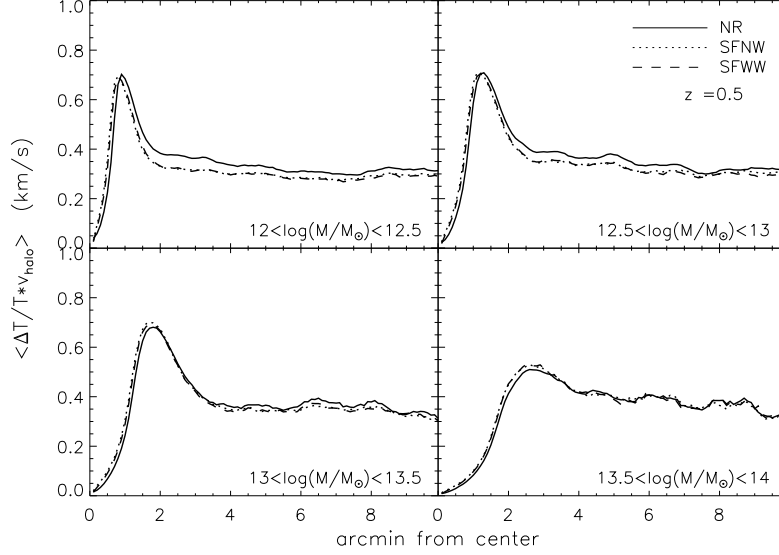


Fig. 7 Same as Fig. 6, but for $z = 0.5$. We find no significant impact of gasphysics on the WHIM contribution.

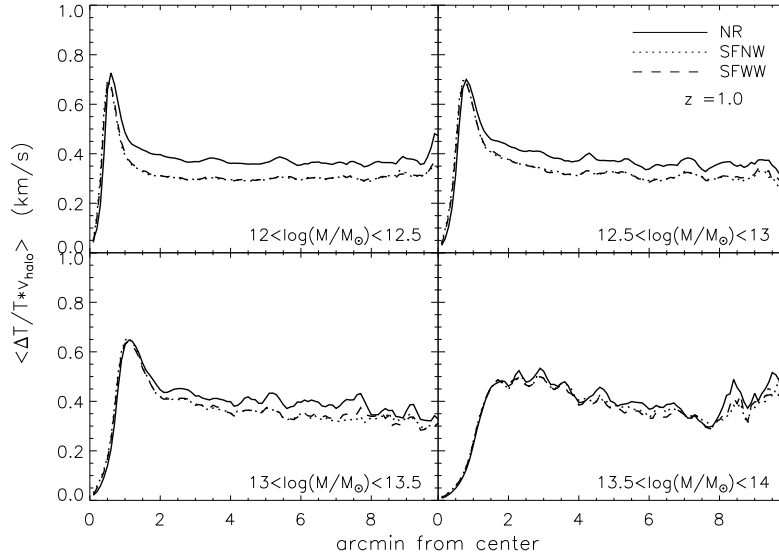


Fig. 8 Same as Figs. 6 and 7, but for $z = 1$. Compared to the cases at lower redshift, the impact of gasphysics is stronger.

θ , reaches the peak at $\theta \sim 1.5\theta_{\text{vir}}$, and then decreases with θ . Towards the halo center, most contribution to the kSZ stacking coming from within the virial radius (Figs. 2 and 3), where the WHIM fraction is low. Therefore we find that the WHIM contribution to the stacking signal decreases to zero toward the center. Around the peak, the WHIM contribution is $\sim 50\%$ – 70% and therefore WHIM is the dominant contribution of the stacking signal. Figure 2 shows that at $\theta \sim 2'$ about 90% of the contribution comes from within projection depth $3r_{\text{vir}}$. In combination with the result in Figure 6, this shows that most of the WHIM is located near the stacked halos. However, even at the peak, contribution from hotter gas is significant. Furthermore, at other θ , the WHIM contribution is in general sub-dominant

($< 50\%$), although still significant. These results imply that it is challenging to properly interpret the stacking result in order to probe missing baryons, since WHIM never overwhelms other contributions to the stacking signal.

These figures also show the dependence of WHIM contribution on gasphysics. Although we do find a visible impact on gasphysics, the impact is usually insignificant at $z \lesssim 0.5$. The impact at higher redshift (e.g. $z = 1$) is larger. For $z = 1$ and mass bin 1, the included gasphysics reduces the WHIM fraction from $\sim 40\%$ to $\sim 30\%$ over a large range of $\theta \sim 2' - 10'$. With increasing mass and deeper potential wells, the impact of gasphysics weakens, as shown in Figure 8. The impact of star formation, cooling and stellar feedback eventually becomes neg-

ligible for halos with mass $\gtrsim 10^{13.5} M_{\odot}/h$ at $z \gtrsim 1$. We caution that AGN feedback is expected to be important for these redshifts and mass range, and therefore may cause non-negligible to significant impact on the kSZ stacking. Investigation on this issue is beyond the scope of this paper.

6 CONCLUSIONS

The kSZ stacking technique is a powerful tool of isolating the weak kSZ effect from overwhelming background and foreground contaminations. Recently the Planck team has applied this technique to Planck data and detected the kSZ effect at $\sim 3\sigma$. An unresolved issue of kSZ stacking is its relation to the baryon budget, namely the relation between kSZ stacking statistics and the amount of baryons in various forms (e.g. WHIM). Through a set of hydrodynamic simulations, we measure the kSZ stacking and its dependence on halo mass, redshift and gas physics. We quantify the contribution from various projection depths to the stacking signal, and the contribution from WHIM. We find that in general the WHIM contribution is significant. The WHIM fraction is about 10% \sim 70%. On one hand, this means that it is indeed promising to probe WHIM and therefore missing baryons through kSZ stacking. On the other hand, this finding means that virialized gas in halos along the LOS is either significant or dominant in the stacked kSZ signal. This complicates the interpretation of the stacking signal as evidence of missing baryons. It is therefore a major challenge to probe WHIM with kSZ. This conclusion is valid for all redshifts and most angular separations to the stacked halos. It also holds with the presence of SN feedback and gas cooling, as verified in our simulations. These findings demand more detailed analysis of the kSZ stacking.

Nonetheless, we caution that these results cannot be directly applied to explain the Planck result. Besides the obvious reason that the Planck result is achieved at an average redshift $z = 0.12$, there are further complexities. To robustly explain the Planck result, we need a realistic mock catalog of galaxies, robust evaluation of velocity reconstruction error, inclusion and evaluation of primary CMB contaminations and aperture statistics. We also need to check the simplified estimation of the mean optical depth τ adopted in the Planck result (Planck Collaboration et al. 2015b), and the estimator of baryon fraction proposed in Hernández-Monteagudo et al. (2015). Furthermore, AGN feedback is known to be significant for the distribution of evolution of baryons and should be appropriately included in the analysis. We leave these issues for further investigation.

Acknowledgements We acknowledge support by the National Natural Science Foundation of China (Grant Nos. 11473053, 11233005, U1331201 and 11121062), the National Key Basic Research Program of China (Grant No. 2015CB857001), and the ‘‘Strategic Priority Research Program the Emergence of Cosmological Structures’’ of the Chinese Academy of Sciences (Grant Nos. XDB09000000 and XDB09010000). The work made use of the High Performance Computing Resource in the Core Facility for Advanced Research Computing at Shanghai Astronomical Observatory.

References

- Bregman, J. N. 2007, *ARA&A*, 45, 221
 Cen, R., & Ostriker, J. P. 1999, *ApJ*, 514, 1
 Cen, R., & Ostriker, J. P. 2006, *ApJ*, 650, 560
 Davé, R., Cen, R., Ostriker, J. P., et al. 2001, *ApJ*, 552, 473
 Fukugita, M., Hogan, C. J., & Peebles, P. J. E. 1998, *ApJ*, 503, 518
 George, E. M., Reichardt, C. L., Aird, K. A., et al. 2015, *ApJ*, 799, 177
 Haehnelt, M. G., & Tegmark, M. 1996, *MNRAS*, 279, 545
 Hand, N., Addison, G. E., Aubourg, E., et al. 2012, *Physical Review Letters*, 109, 041101
 Hernández-Monteagudo, C., Ma, Y.-z., Kitaura, F.-S., et al. 2015, arXiv:1504.04011
 Planck Collaboration, Aghanim, N., Arnaud, M., et al. 2015a, arXiv:1507.02704
 Planck Collaboration, Ade, P. A. R., Aghanim, N., et al. 2015b, arXiv:1504.03339
 Sayers, J., Mroczkowski, T., Zemcov, M., et al. 2013, *ApJ*, 778, 52
 Shao, J., Zhang, P., Lin, W., Jing, Y., & Pan, J. 2011, *MNRAS*, 413, 628
 Sievers, J. L., Hlozek, R. A., Nolta, M. R., et al. 2013, *J. Cosmol. Astropart. Phys.*, 10, 60
 Springel, V. 2005, *MNRAS*, 364, 1105
 Springel, V., Yoshida, N., & White, S. D. M. 2001, *New Astron.*, 6, 79
 Sunyaev, R. A., & Zeldovich, I. B. 1980, *MNRAS*, 190, 413
 Sunyaev, R. A., & Zeldovich, Y. B. 1970, *Ap&SS*, 7, 3
 Sunyaev, R. A., & Zeldovich, Y. B. 1972, *Comments on Astrophysics and Space Physics*, 4, 173
 White, M., Hernquist, L., & Springel, V. 2002, *ApJ*, 579, 16
 Zeldovich, Y. B., & Sunyaev, R. A. 1969, *Ap&SS*, 4, 301